Pathogenic fungi neutralize plant-derived ROS via Srpk1 deacetylation

Ning Zhang, Fangjiao Lv, Fahui Qiu, Dehai Han, Yang Xu, and Wenxing Liang

Appendix Contents

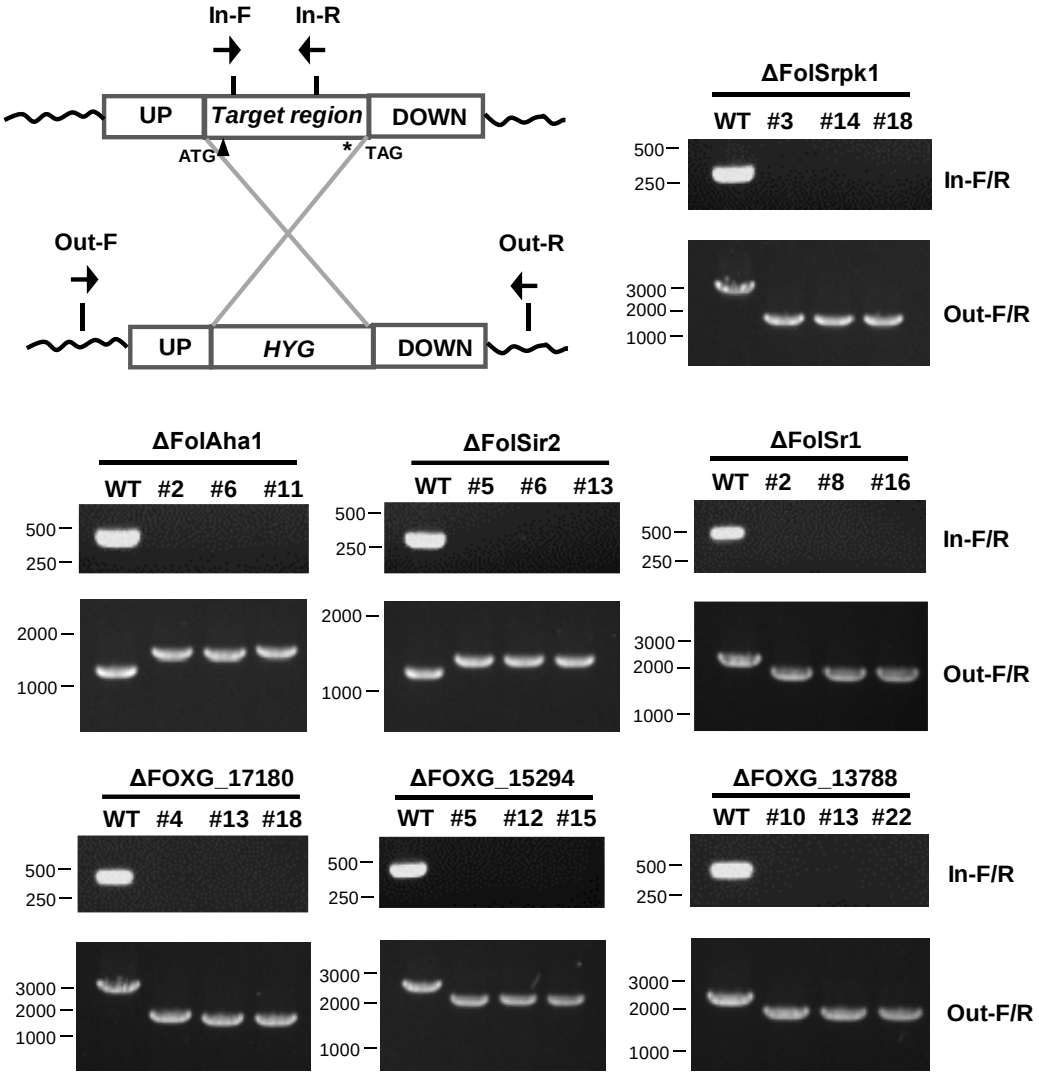

Appendix Figure S1. Generation of mutant strains of the target genes in *Fol*.

Genomic DNA was analyzed by PCR with the indicated primer pairs.

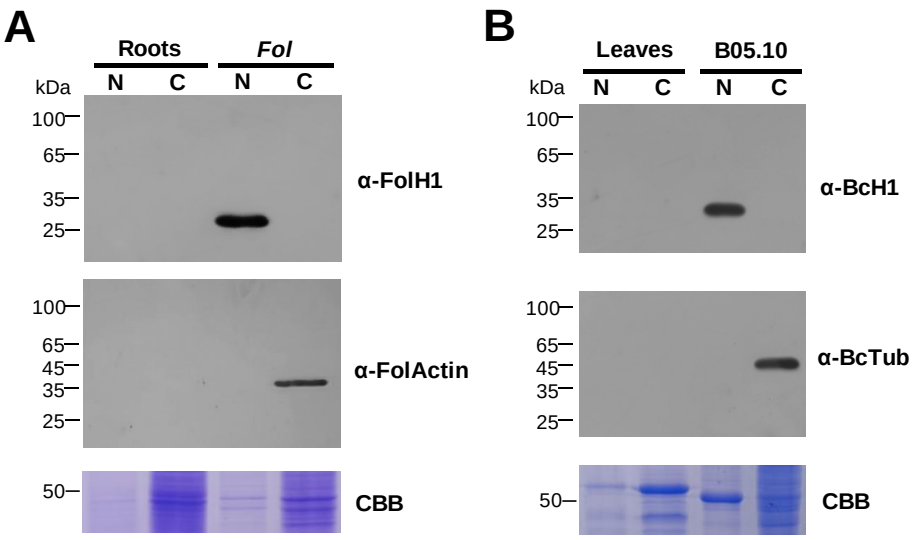

Appendix Figure S2. Specificity validation of fractionation control antibodies.

A Validation of anti-FolH1 and anti-FolActin. Equal amount of the nuclear and cytoplasm proteins from tomato roots and *Fol* was separated by SDS-PAGE, and histone H1 and actin of *Fol* were detected by the indicated antibodies. CBB staining shows protein loading to each lane.

B Validation of anti-BcH1 and anti-BcTub. Equal amount of the nuclear and cytoplasm proteins from tomato leaves and *B05.10* was separated by SDS-PAGE, and histone H1 and tubulin of *B05.10* were detected by the indicated antibodies. CBB staining shows protein loading to each lane.

Data information: For A and B, each gel shown is a representative experiment carried out three times.

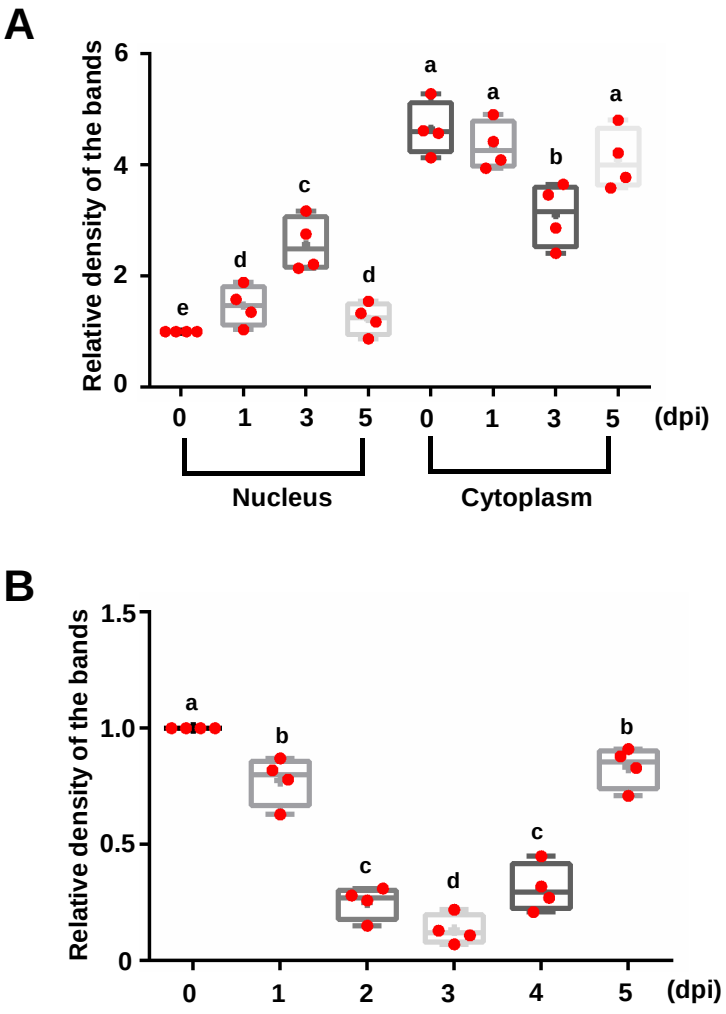

Appendix Figure S3. Quantification of the intensity of cytoplasmic and nuclear FolSrpk1-GFP proteins in Fig 1E (A) and Fig 2J (B).

Statistical significance was revealed by one-way ANOVA (mean ± SE of 4 independent biological replicates). The whiskers of the boxplots indicate the upper and lower quartiles, the boxes indicate the interquartile range, and the plus sign indicates the mean.

FolSrpk1 (80.2%)

MAHSPSSSSVDDAAENTADEEDSEDYCKGGYHPVQVGEKFKDGKYTVVRK
LGWGHFSTVWLSRDNTNGKHVALKVVRSAAHYTETAIDEIKLLNKIVQAKPD
HPGRKHVVSLLDSFEHKGPHGTHVCMVFEVLGENLLGLIKRWNHRGIPMPL
VKQITKQVLLGLDYLHRECGIIHTDLKPENVLIEIGDVEQIVKRVVKPESAEKE
NNRNGRRRRRTLITGSQPLPSPLNTSFNQSNLFPSPNTHSSLAGVLNEAGK
SSKEASPKPSDDAQKQREKSADLLSREVSGISLDKSNSPSASTGEKRKAED
AHAFDVISVKIADLGNACWVNHHFTNDIQTRQYRSPEVILGSKWGASTDVW
SMAAMVFELITGDYLFDPQSGTKYGKDDDHIAQIIELLGPFPKSLCLSGKWS
QEIFNRKGELRNIHRLRHWALPDVLREKYHFKEDEAKRIADFLTPMLELVPE
KRANAGGMAGHVWLEDTPGMKGLKIEGLEVGGRGEGIDGWATEVRKR

Appendix Figure S4. Coverage of the identified peptides of FolSrpk1 in MS analysis.

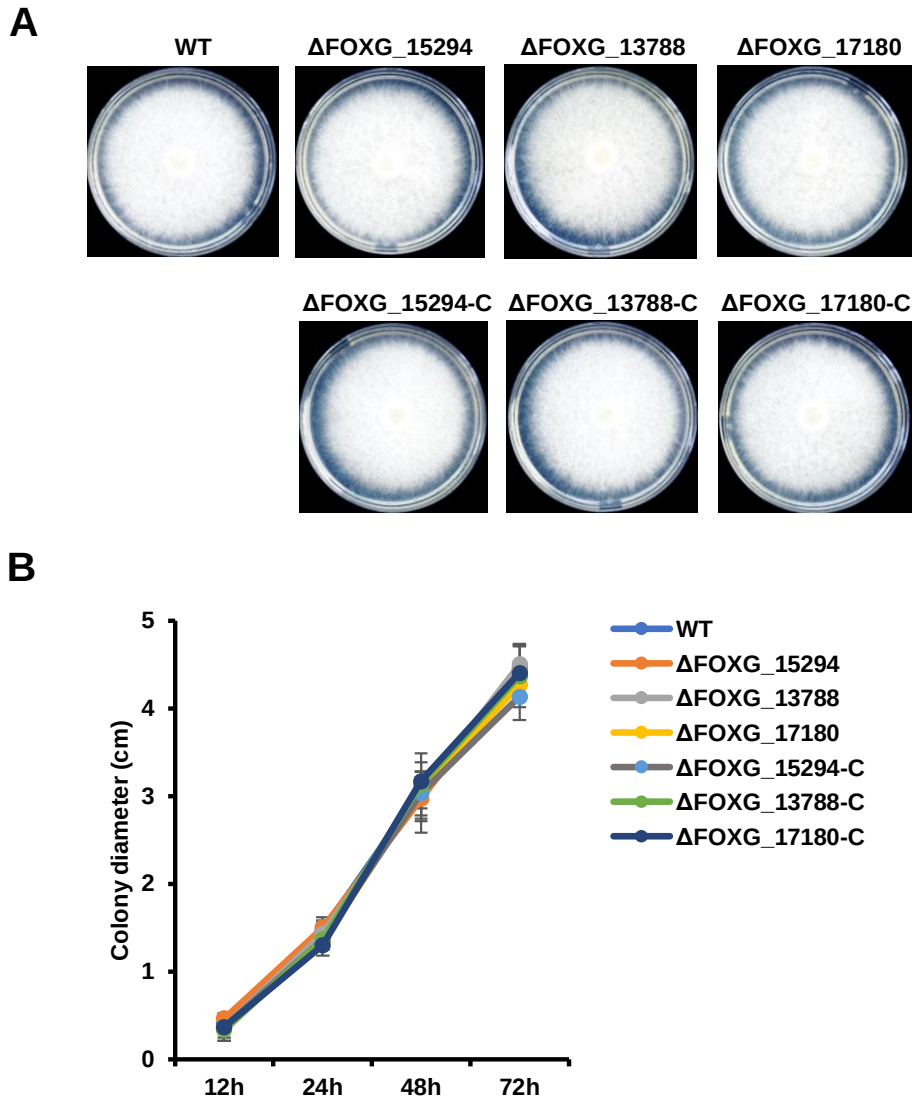

Appendix Figure S5. Phenotypic analysis of the WT and mutant strains.

A Mycelial growth of the WT and mutant strains on PDA plates. Images were taken 3 days after cultivation.

B Colony diameter of the indicated strains on PDA plates 12 h-72 h after cultivation. The data are the means ± SDs (n = 3).

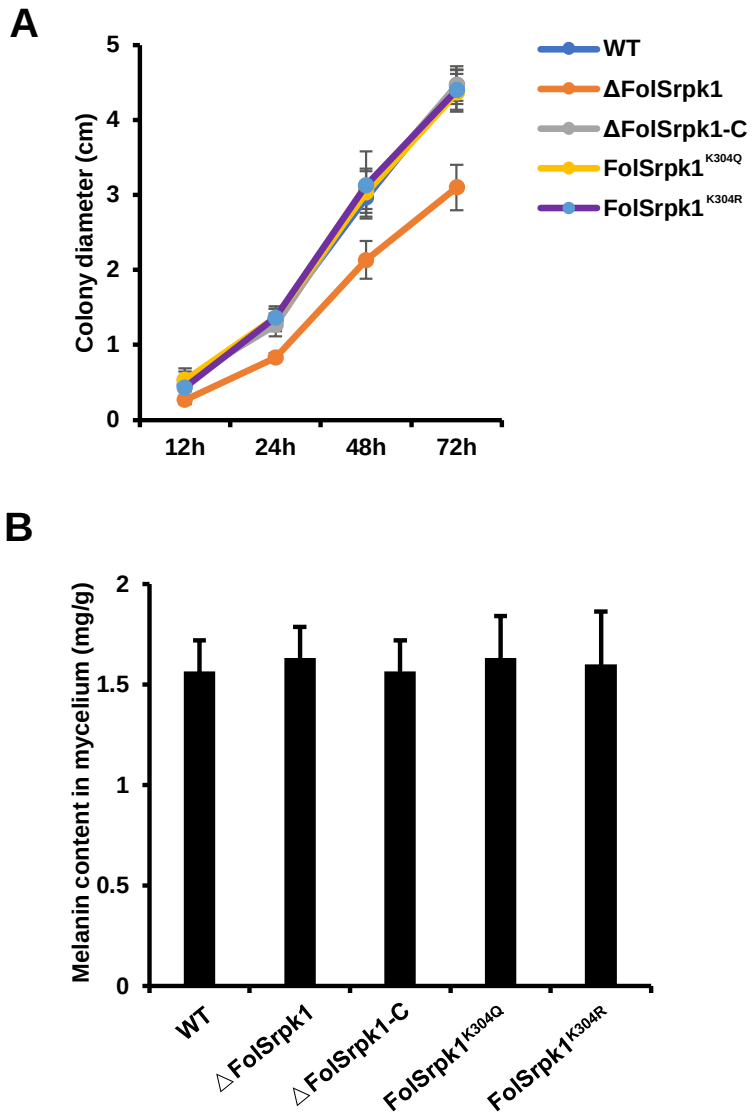

Appendix Figure S6. Phenotypic analysis and melanin accumulation of the WT and mutant strains.

A Colony diameter of the indicated strains on PDA plates 12 h-72 h after cultivation. The data are the means ± SDs (n = 3).

B Quantification of melanin of the indicated strains on PDA plates 3 days after cultivation. The data are the means ± SDs (n = 3).

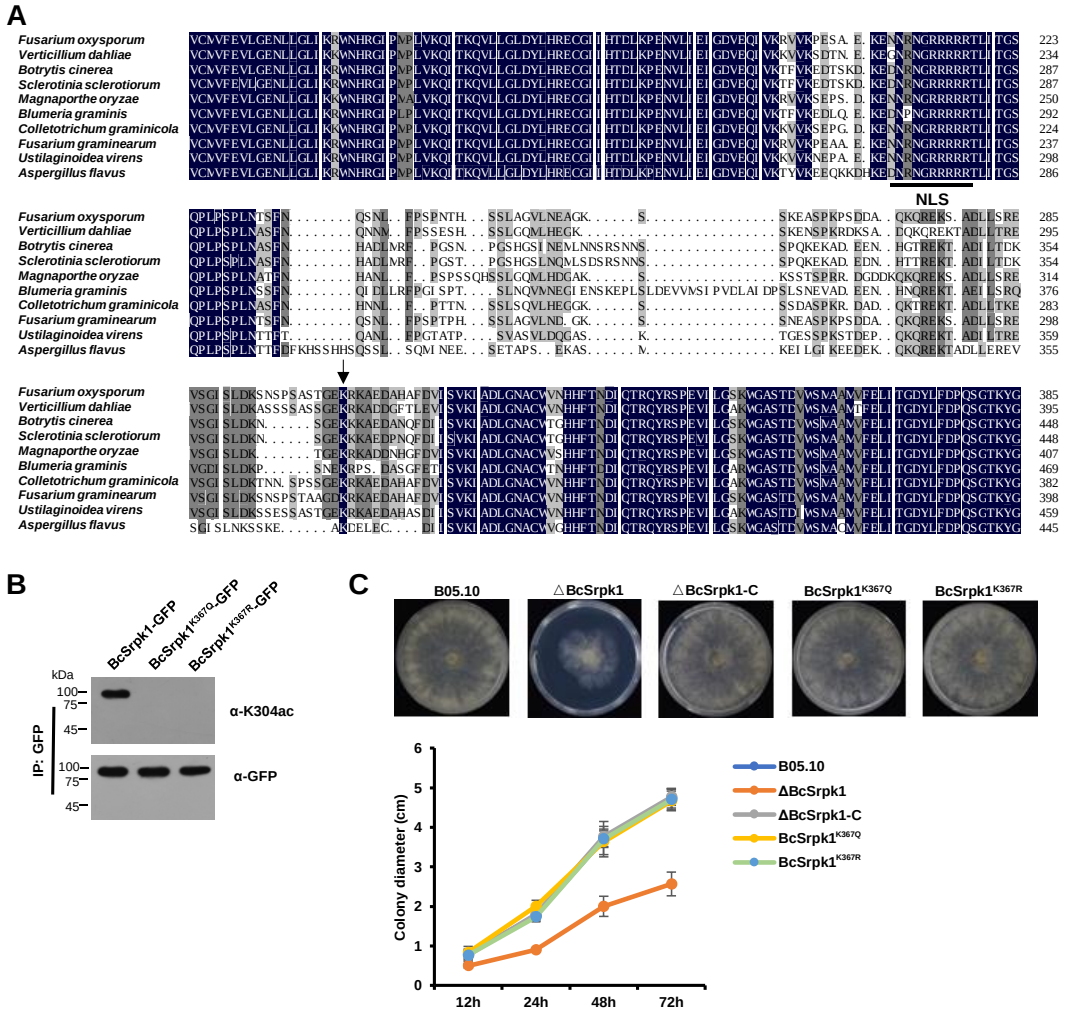

Appendix Figure S7. Conservation of the NLS and K304 of FolSrpk1 in plant fungal homologs.

A Sequence alignment of FolSrpk1 with its homologs. The NLS region was marked with a line. Arrowhead indicates the conserved acetylation site of K304. The FolSrpk1 homologs were *F. oxysporum* FOXG_15645, *V. dahliae* VDAG_01669, *B. cinerea* Bcin08g03050, *S. sclerotiorum* SS1G_03277, *M. oryzae* MGG_10596T1, *B. graminis* BLGH_02186, *C. graminicola* GLRG02654:EFQ26834, *F. graminearum* FGRAMPH1_01G11331, *U. virens* UV8b_3406 and *A. flavus* AFLA_039070.

B Acetylation of WT and K367 mutant BcSrpk1 proteins. BcSrpk1-GFP proteins pulled

down from the indicated samples with GFP-Trap beads were probed with anti-K304ac and anti-GFP antibodies, respectively.

C Mycelial growth and colony diameter of the indicated strains on PDA plates. Images were taken 3 days after cultivation. Colony diameter was measured 12 h-72 h after cultivation. The data are the means ± SDs (n = 3).

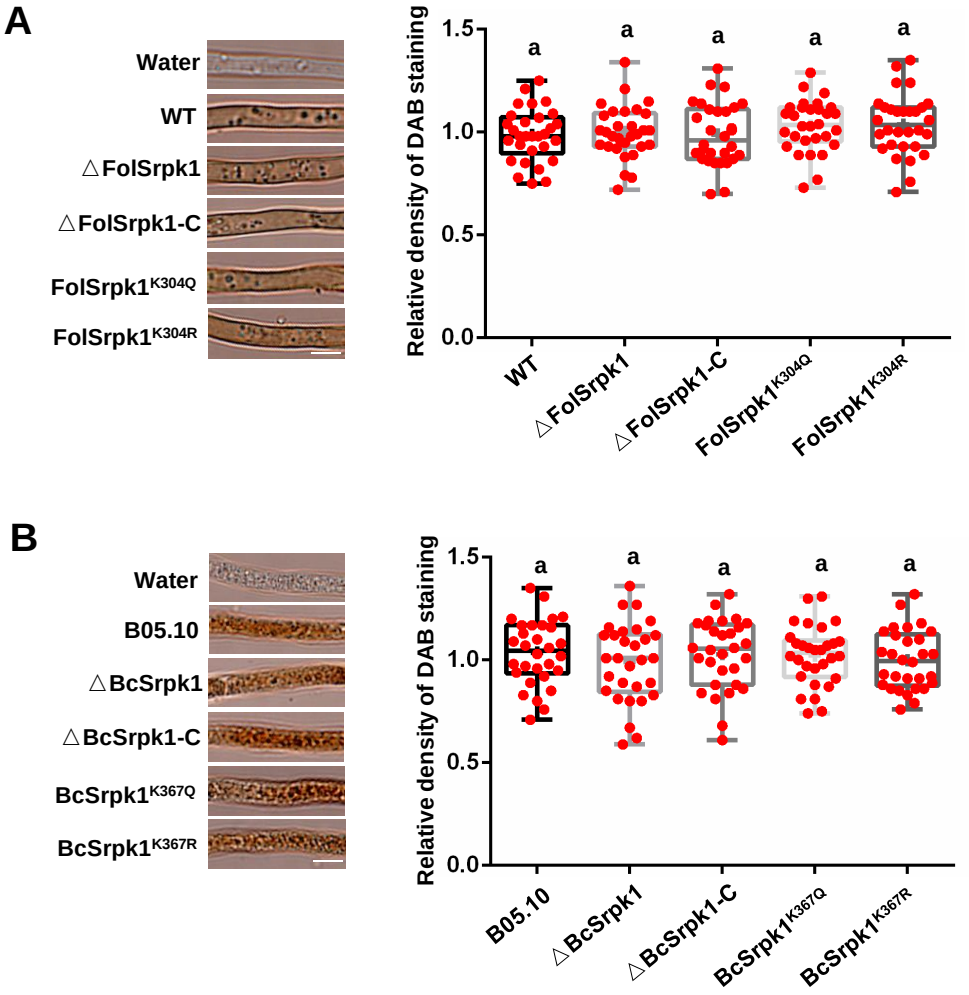

Appendix Figure S8. I*n situ* H_2O_2 accumulation of the WT and mutant strains on PDA plates.

A H_2O_2 accumulation of the WT and FolSrpk1 mutant strains on PDA plates.

B H_2O_2 accumulation of the WT and BcSrpk1 mutant strains on PDA plates. DAB staining was performed as described in Materials and Methods. Images were taken and the relative mean pixel intensity was determined using the ImageJ software. The calculation was from three independent replicates with ten hyphae per replicate. The whiskers of the boxplots indicate the upper and lower quartiles, the boxes indicate the interquartile range, and the plus sign indicates the mean.